Ab Initio Study of the Basic Hydrolysis of the Pyrazolidinone Ring

Miguel Coll,* Juan Frau, Francisco Muñoz, and Josefa Donoso

Departament de Química, Universitat de les Illes Balears, Ctra. Valldemossa, Km 7.5, 07071 Palma de Mallorca, Spain

Received: August 12, 1997; In Final Form: December 17, 1997

A complete study of basic hydrolysis of the pyrazolidinone ring by ab initio calculations at RHF/6-31+G*//RHF/6-31+G* and MP2/6-31+G*//MP2/6-31+G* has been carried out. The alkaline hydrolysis has been studied through a B_{AC2} mechanism, characterized by a nucleophilic attack of the hydroxyl group on the carbonyl of the γ-lactam ring, formation of the tetrahedral intermediate, and cleavage of the C_2N_3 bond to yield the final reaction product. In the gas phase, the interaction of OH^- with the carbonyl carbon to form a tetrahedral intermediate takes place without any barrier height. Two possible mechanisms have been considered for the transfer of the hydroxyl hydrogen to the nitrogen of the γ-lactam: a stepwise mechanism involving the cleavage of the C_2N_3 bond and subsequent transfer of the hydrogen to the γ-lactam nitrogen and a concerted mechanism. The MP2/6-31+G*//MP2/6-31+G* barrier heights are 32.72 and 25.64 kcal/mol, respectively. The elimination reaction, which in the gas phase may interfere with the nucleophilic attack, has also been studied.

Introduction

Since its discovery, at the end of the decade of the 1920s, up to the present, the β-lactam antibiotics have been widely used in the treatment of bacterial diseases.[1] Nevertheless, an increase in the number of strains resistant to the former antibiotics has brought about the need of new compounds showing antibacterial activity.

The discovery at the end of the 1980s of lactivicine,[2] a five-membered lactam ring, together with the design of 1,2-pyrazolidinone bicyclic derivatives, such as the LY1730313,[3,4] has spurred interest in searching γ-lactam compounds endowed with antibacterial activity.[5]

Since the first theoretical works by Boyd[6] in which different structural parameters regarding the β-lactam antibiotics were related to both their chemical and antibacterial activities, numerous theoretical studies have been performed on the structure and reactivity of these compounds.[7−18] Due to the similarity between the enzymatic acylation mechanism and the alkaline hydrolysis,[19] several authors have suggested that the basic hydrolysis constant of the β-lactam carbonyl is an important factor related to antibacterial activity.[20] Although the basic hydrolysis of some γ-lactam compounds has been studied by experimental methods (revealing, in some cases, a certain correlation between reaction rate and antimicrobial activity),[21] up to the present there are no theoretical studies on the reactivity of γ-lactam compounds.

In the present article a wide study of the basic hydrolysis of the pyrazolidinone ring is carried out. This compound has been chosen as a model since the aza-γ-lactam compounds present both the adequate combination of chemical stability and the acylation capacity to possess antimicrobial activity.[5] The basic hydrolysis has been studied through a B_{AC2} mechanism, characterized by a nucleophilic attack on the γ-lactam carbonyl, further formation of a tetrahedral intermediate, and, finally, cleavage of the C_2N_3 bond and subsequent hydrogen transfer to yield the final reaction product. This mechanism is analogous to that described for β-lactam antibiotics.[12] In the gas phase, the OH^- attack on a carbonyl compound may give rise to the interaction between the hydroxyl ion and a hydrogen, with further elimination of the former hydrogen and formation of a water molecule.[13,14,16] This reaction has been also considered in this study.

* Corresponding author. e-mail: dqumcp4@ps.uib.es.

Methodology

The ab initio calculations on the pyrazolidinone ring together with the structures yielded in the studied reactions were initially carried out at the RHF/6-31+G*//RHF/6-31+G* level, which includes polarized and diffuse functions on heavy atoms. The incorporation of diffuse functions is especially relevant in the calculations of anionic systems.[22]

All the structures have also been optimized using Møller−Plesset's perturbation theory,[23] as implemented by Pople et al.,[24] at the MP2 level (MP2/6-31+G*//MP2/6-31+G*). Henceforward, RHF and MP2 stand for RHF/6-31+G*//RHF/6-31+G* and MP2/6-31+G*//MP2/6-31+G*, respectively. All the energies include the ZPE correction. For MP2 energies we use the HF ZPEs scaled by 0.8929 as recommended by Pople et al.[25]

All the transition states are characterized by exhibiting just one imaginary frequency, greater than 100i cm^{-1} in all cases. IRC calculations of the former transition states were performed to confirm all the intermediates proposed in this study.

The calculations were performed on an ALPHA DEC 10620 AXP computer running the GAMESS US program [26] as modified by Schmidt et al.[27]

Results and Discussion

Scheme 1 shows the B_{AC2} mechanism considered for the pyrazolidinone hydrolysis and the numbering of the system. This mechanism basically implies the nucleophilic addition of the hydroxyl ion to the γ-lactam ring, further formation of the tetrahedral intermediate, and subsequent cleavage of the C_2N_3 bond. A similar mechanism has been considered for carbonyl compounds, including β-lactam compounds.[12,13,15−18]

S1089-5639(97)02625-X CCC: $15.00
Published on Web 06/29/1998

SCHEME 1: Alkaline Hydrolysis (B_{AC2} Mechanism) of the Pyrazolidinone Ring

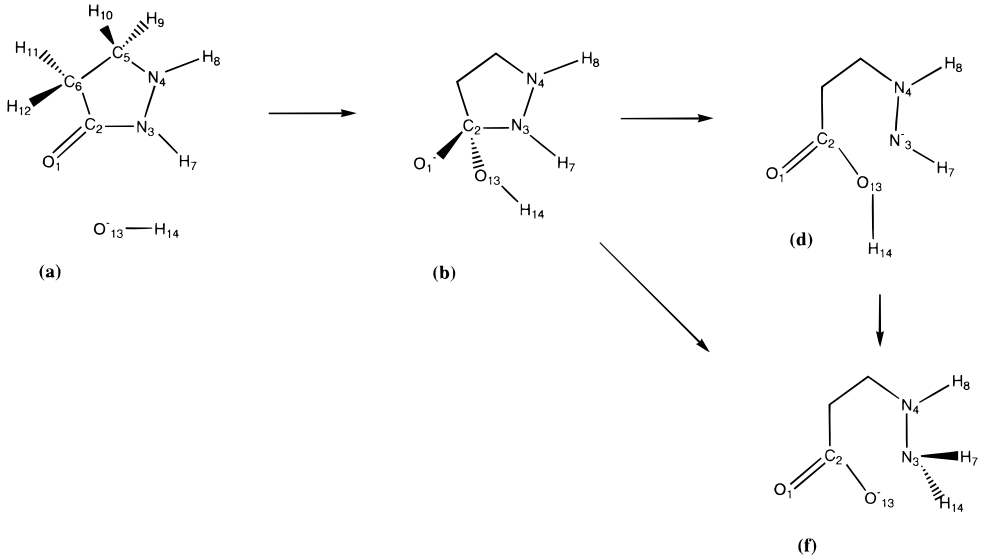

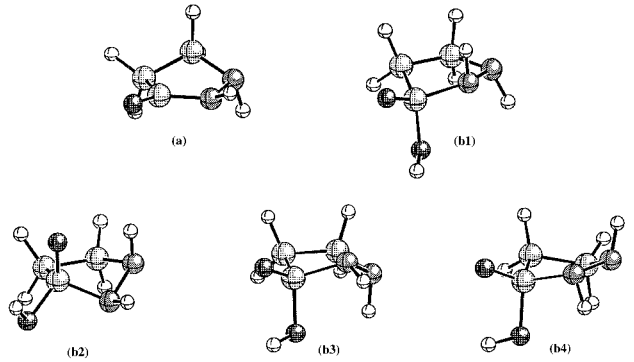

Figure 1. Structures corresponding to the pyrazolidinone ring (**a**) and to the tetrahedral intermediates (**b1**, **b2**, **b3**, and **b4**).

Pyrazolidinone Ring (a). Geometric parameters and total energy of the pyrazolidinone ring (Figure 1) are depicted in Table 1. The MP2 calculation performed on this structure slightly increases all bond distances relative to the RHF calculation. This increase is between 0.03 and 0.01 Å, except for C_5C_6 and C_2C_6 distances, which only increase 0.003 Å. Variation of both bond and dihedral angles is virtually nonexistent.

Tetrahedral Intermediate (b). The attack of the hydroxyl ion on structure **a** by its bottom face yields four possible structures of the tetrahedral intermediate (Figure 1), whose geometric parameters and energies are shown in Table 1. These different conformations of the five-membered ring are characterized by the different orientations of H_7 and H_8 atoms. The lowest energy structure (**b1**) presents H_7 and H_8 at the axial (up)−axial (down) position. The equatorial (up)−axial (up) (**b2**), the equatorial (down)−axial (down) (**b3**), and axial (down)−axial (up) (**b4**) are also possible. There are also small differences regarding the distance from O_{13} to C_2 (from 1.451 Å in **b1** to 1.486 Å in **b3**, larger than that observed in the β-lactam ring, 1.427 Å[13]). In general, all bond lengths vary between 0.01 and 0.05 Å for the different conformers.

The MP2 calculations emphasize the differences between the bond lengths in the different conformations. Furthermore, these calculations lengthen all the bond distances between 0.03 and 0.01 Å, except for C_5C_6 and C_2C_6 which increase something less (between 0.005 and 0.001 Å).

The bond angles of the five-membered ring slightly vary from one structure to the other, depending on the ring strain. In the $N_3N_4C_5$ angle this variation can reach up to 8° (between structures **b1** and **b2**).

Important differences in the $C_2N_3-N_4C_5$ dihedral angle may be found in the different structures. This dihedral angle shows the relative position of C_2 in relation to the plane formed by the N_3, N_4, and C_5 atoms. Structure **b4** presents the lowest value for this parameter, therefore being the most planar structure. In RHF calculations, C_2 is located below the plane, with an angle of −8.5°. In **b2** the former carbon is also located below the plane, getting a much larger dihedral (−53.4°). In structures **b1** and **b3** the situation is reversed, and C_2 appears above the plane (dihedrals of 24.7° and 49.6°, respectively). MP2 calculations tend to increase these values; thus, the structures calculated by this method are less planar. However, the variation of these dihedral angles is relatively small (between 0.6° and 1.4°).

Energy differences of these structures are very small, with a maximum value of 3.50 kcal/mol between structures **b1** and **b4**. The stabilization energy, with regard to the reactants (pyrazolidinone and hydroxyl ion), is important (33.04 kcal/mol, MP2), although smaller than the analogue reaction of the β-lactam ring.[13]

The addition of the nucleophile to the carbonyl group takes place without energy activation (likewise, the analogue reaction of the β-lactam ring[12,13,17]), which has been proved by withdrawing the OH^- group from C_2 in the lowest energy structure of the tetrahedral intermediate **b1**. If the OH^- group is withdrawn from C_2 following a perpendicular path to the ring plane, a monotonic increase of energy is observed from the tetrahedral intermediate to reactants. Hence, there are no intermediates or transition states between the reagents and the tetrahedral intermediate.

Ring Opening. The lowest energy tetrahedral intermediate (**b1**) evolves through the ring-opening step to transition state **c1** (Figure 2). The energy increase corresponding to this process is 27.26 kcal/mol by RHF calculations and slightly larger, 32.72 kcal/mol, by MP2 calculations. This transition state is characterized by a C_2N_3 distance of 2.477 and 2.664 Å in RHF and MP2 calculations, respectively (Table 2). Vibrational analysis of the former structure presents just an imaginary frequency in which C_2 and N_3 atoms are involved (see Table 2). IRC

TABLE 1: Main Geometric Parameters and Energy of the Pyrazolidinone Ring (a) and the Tetrahedral Intermediates (b1−b4)[a]

	structure **a**[b]		structure **b1**		structure **b2**		structure **b3**		structure **b4**	
	RHF	MP2	RHF	MP2	RHF	MP2	RHF	MP2	RHF	MP2
O_1C_2	1.1944	1.2283	1.2891	1.2996	1.3082	1.3254	1.2864	1.2945	1.2873	1.2954
C_2N_3	1.3655	1.3793	1.4909	1.5129	1.4920	1.5150	1.4798	1.4989	1.5102	1.5337
N_3N_4	1.4085	1.4293	1.4180	1.4453	1.4296	1.4613	1.4271	1.4583	1.4314	1.4617
N_4C_5	1.4688	1.4847	1.4811	1.5067	1.4655	1.4845	1.4668	1.4861	1.4663	1.4842
C_5C_6	1.5303	1.5269	1.5309	1.5260	1.5447	1.5436	1.5443	1.5397	1.5185	1.5144
C_2C_6	1.5206	1.5236	1.5528	1.5539	1.5567	1.5530	1.5548	1.5544	1.5487	1.5489
C_2O_{13}			1.4506	1.5006	1.4282	1.4643	1.4857	1.5589	1.4732	1.5424
$O_{13}H_{14}$			0.9482	0.9779	0.9476	0.9777	0.9478	0.9775	0.9479	0.9782
$O_1C_2N_3$	125.5	125.5	113.4	114.2	113.8	114.2	116.1	116.8	116.4	116.8
$O_1C_2C_6$	128.1	128.4	118.2	119.4	114.7	115.0	119.9	121.2	118.0	119.4
$C_2N_3N_4$	113.6	113.7	108.5	107.1	103.1	101.2	106.2	104.9	110.4	109.2
$N_3N_4C_5$	104.7	103.6	108.7	107.8	100.8	99.3	101.2	100.0	107.2	106.3
$O_{13}C_2N_3$			104.7	102.8	106.9	105.8	105.6	104.3	104.1	102.8
$H_{14}O_{13}C_2$			102.5	99.3	101.9	98.8	100.9	96.7	101.2	97.6
$O_1C_2-N_3N_4$	188.8	189.3	198.8	165.6	288.1	291.8	183.9	180.5	215.5	213.1
$H_7C_2-N_3N_4$	215.4	215.8	243.7	246.0	246.6	249.3	118.4	114.7	115.6	112.5
$H_8C_2-N_3N_4$	32.4	33.0	31.4	31.6	335.5	336.0	25.4	25.1	328.2	327.8
$C_2N_3-N_4C_5$	13.1	12.1	24.7	26.1	306.6	305.3	49.6	50.2	351.5	350.5
$O_1C_2-C_5C_6$	294.9	294.0	311.1	316.7	257.3	254.1	306.0	308.8	320.7	325.2
$O_{13}C_2-N_3N_4$			74.8	70.4	164.8	168.3	61.6	58.5	93.9	91.9
energy	−376.2145031	−377.3432092	−376.2606804	−377.4016140	−376.2569753	−377.3993563	−376.2553172	−377.3985499	−376.2538568	−377.3958803
ZPE	0.116475	0.104000	0.122919	0.109754	0.123526	0.110296	0.122925	0.109760	0.122739	0.109594
no. imag freq	0		0		0		0		0	

[a] Bond lengths in angstroms, bond and dihedral angles in degrees, and energy in hartrees. [b] For structure **a**, energy and ZPE is the addition of pyrazolidinone and OH^- energies.

Figure 2. Structures corresponding to the transition states, intermediate, and different conformations of the final product of the alkaline hydrolysis.

calculations on this transition state show that the reverse pathway ends back at the tetrahedral intermediate (**b1**) and the forward pathway ends at structure **d** (Figure 2, Table 2). In structure **d** the C_2N_3 bond is completely cleft, and H_{14} is still linked to O_{13} and very far from N_3. The C_2N_3 distance for this intermediate is of 3.858 Å in RHF calculations and smaller by MP2 calculations (3.772 Å). The energy difference between transition state **c1** and intermediate **d** is very small (−2.90 kcal/mol in MP2 calculations).

A rotation of the OH^- group should be carried out in order to get a better orientation of this group, allowing the direct transfer of the proton of the carboxyl group to N_3. The activation energy implied in this rotation is very small. When H_{14} is correctly oriented, it is transferred directly to the amino group. Because of that, it has been impossible to characterize the transition state corresponding to this rotation (**e**, Figure 3). This reaction pathway that occurs through the transition state **c1** and the intermediate **d** implies a stepwise mechanism characterized by a cleavage of the tetrahedral intermediate with further transfer of the acidic proton to yield the carboxylate anion.

The ring opening and transfer of acidic proton could also take place through a concerted mechanism. The intermediate **b2** presents the best spatial arrangement to promote this process. The study of the reaction pathway from this tetrahedral intermediate yielded a transition state **c2** with one imaginary vibrational frequency (314.97i cm^{-1}) in which C_2, N_3, and H_{14} are involved. The activation energy of this process is lower than that obtained in the previous nonconcerted process; however, it still remains considerably high (20.13 kcal/mol by RHF calculations and 25.64 kcal/mol by MP2). In this transition state H_{14} is located only at 2.211 Å from N_3 according to the RHF results and at 2.044 Å according to MP2 calculations. This short distance implies the existence of an intramolecular hydrogen bond which, probably, causes the greater stability of this transition state. The C_2N_3 distance is smaller than in the structure **c1** (2.393 Å instead of 2.665 Å), and the spatial orientation of the carboxyl group is very different, as shown in Figure 2. IRC calculations end at the tetrahedral intermediate in the reverse pathway and directly at the final reaction product (**f**) in the forward pathway. Hence, the concerted process is the most favorable pathway for the reaction.

Three conformations have been identified for the final reaction product (**f1**, **f2**, and **f3**, Figure 2, Table 3). The lowest energy structure (**f1**) displays an intramolecular hydrogen bond of 2.139 Å (RHF) and 1.969 Å (MP2) between the O_{13} and H_8 atoms. In structure **f2** an intramolecular hydrogen bond also appears, now between the O_{13} and H_{14} atoms, with a distance of 1.940 Å (RHF) and 1.854 Å (MP2). It presents an energy slightly

TABLE 2: Main Geometric Parameters and Energy of the Different Transition States and Intermediates of the B_{AC2} Reaction[a]

	structure **c2**		structure **c1**		structure **d**	
	RHF	MP2	RHF	MP2	RHF	MP2
O_1C_2	1.2066	1.2311	1.2015	1.2257	1.2014	1.2346
C_2N_3	2.2314	2.3928	2.4765	2.6642	3.8584	3.7723
N_3N_4	1.4433	1.4668	1.4436	1.4641	1.4498	1.4624
N_4C_5	1.4429	1.4528	1.4560	1.4614	1.4377	1.4593
C_5C_6	1.5536	1.5548	1.5438	1.5492	1.5598	1.557
C_2C_6	1.5218	1.5132	1.5018	1.4990	1.4965	1.4781
C_2O_{13}	1.3650	1.3919	1.3450	1.3752	1.3339	1.3687
$O_{13}H_{14}$	0.9524	0.9923	0.9495	0.9795	0.9509	0.9808
$O_1C_2N_3$	113.4	116.3	112.4	111.6	153.9	167.1
$O_1C_2C_6$	120.9	121.2	125.0	126.5	125.9	128.0
$C_2N_3N_4$	90.8	85.7	91.0	84.7	56.0	60.3
$N_3N_4C_5$	103.9	103.4	111.5	109.1	111.8	110.3
$O_{13}C_2N_3$	93.1	88.1	88.9	90.3	77.3	73.0
$H_{14}O_{13}C_2$	103.7	97.4	106.6	104.1	107.4	104.6
O_1C_2-N_3N_4	296.9	304.2	189.6	180.3	337.1	292.4
H_7C_2-N_3N_4	251.4	255.4	248.5	245.9	326.7	319.7
H_8C_2-N_3N_4	334.8	334.8	28.9	28.0	35.1	34.6
C_2N_3-N_4C_5	307.2	305.4	36.6	45.3	49.0	47.7
O_1C_2-C_5C_6	239.2	235.1	305.6	304.0	114.1	100.0
$O_{13}C_2$-N_3N_4	172.5	180.4	67.0	57.1	111.3	89.5
energy	−376.2214263	−377.3553996	−376.2135161	−377.3461642	−376.2170447	−377.3510242
ZPE	0.120055	0.107197	0.119205	0.106438	0.119477	0.106681
no. of imag freq	1 (314.97*i*)		1 (135.61*i*)		0	

[a] Bond lengths in angstroms, bond and dihedral angles in degrees, energy in hartrees, and imaginary frequencies in cm^{-1}.

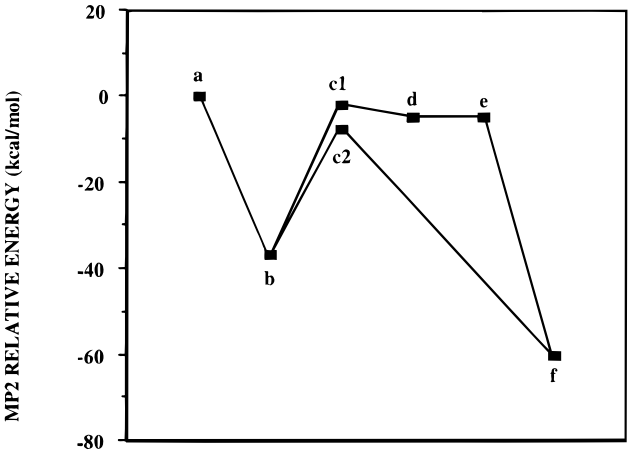

Figure 3. Reaction profile of the alkaline hydrolysis of the pyrazolidinone ring.

higher than **f1**. The energy difference between them is very small, just 0.83 kcal/mol by RHF calculation and 1.15 kcal/mol by MP2. Structure **f3** is found to be totally extended and does not present any intramolecular hydrogen bonds. The energy difference between the less stable structure **f3** and the most stable structure **f1** is 4.83 kcal/mol (RHF) and 6.38 kcal/mol (MP2).

Reaction Profile. In Table 4 and Figure 3 are represented the relative energies (MP2) of the different intermediates and transition states obtained for the basic hydrolysis of pyrazolidinone. The final product of the alkaline hydrolysis reaction (**f**) is more stable than the initial reagents ($\Delta E = -50.79$ kcal/mol, RHF and $\Delta E = -56.71$ kcal/mol, MP2). A same order value ($\Delta E = -76.61$ kcal/mol) was obtained in the theoretical study of the analogous reaction of the azetidin-2-one ring.[15] As it has been shown, there are two ring-opening mechanisms: a direct process, concerted, in which the transition state **c2** yields directly the final reaction products, and another more complex process in which the transition state **c1** produces an intermediate (**d**) which should overcome a small rotation barrier of the hydroxyl group to generate the final product. The barrier height of the direct process through the transition state **c2** is 7.08 kcal/mol smaller than the stepwise mechanism in MP2 calculations. It favors the direct process as the most likely pathway. Similar concerted processes have been described by Pitarch et al.,[17] Smeyers et al.,[11] and our research group for the alkaline hydrolysis of the β-lactam ring.[18]

As recently shown by theoretical methods,[18] inclusion of the solvent effects in the basic hydrolysis of the β-lactam cycle only has relevant effects on the formation of the tetrahedral intermediate. It is well-known that in gas the phase the formation of tetrahedral intermediate proceeds without barrier heights. This has been observed independently of the level of theory (semiempirical, HF, MP2).[12,17,18,28] In addition, the tetrahedral intermediate is very stable compared to the reagents; this is due to the fact that the negative charge of the system is more stabilized in the β-lactam ring than in the hydroxyl ion. The inclusion of the solvent produces two important effects on the formation of the tetrahedral intermediate. It gives rise to a great stabilization of the reagents, especially of the hydroxyl, in such a way that these are more stable than the tetrahedral intermediate; this process now shows a barrier height ca. 13−20 kcal/mol, depending on the level of theory.[13,18]

The evolution of the tetrahedral intermediate toward final products through ring opening and transfer of hydrogen to the β-lactam nitrogen is slightly affected by the solvent, showing in all cases activation energies lower than 11 kcal/mol.[13,18] This clearly shows that in solution the limiting step is the formation of the tetrahedral intermediate and not its cleavage as it happens in the gas phase. These theoretical results are in agreement with those experimentally obtained by Bowden and Bromley,[29] which prove that basic hydrolysis of β-lactam rings presents an activation energy of 16 kcal/mol and the limiting step is the formation of the tetrahedral intermediate.

In the present study we have obtained a barrier height of 25.64 kcal/mol for the cleavage of the tetrahedral intermediate, and according to the studies carried out on β-lactam compounds, this value would be practically unaltered by the presence of solvent.

TABLE 3: Main Geometric Parameters and Energy of the Different Conformations of the Final Product of the B_{AC2} Reaction[a]

	structure **f1**		structure **f2**		structure **f3**	
	RHF	MP2	RHF	MP2	RHF	MP2
O_1C_2	1.2340	1.2631	1.2328	1.2636	1.2365	1.2677
C_2N_3	3.6333	3.5458	3.5430	3.5222	4.4790	4.4671
N_3N_4	1.4203	1.4514	1.4170	1.4446	1.4162	1.4423
N_4C_5	1.4545	1.4663	1.4609	1.4743	1.4647	1.4737
C_5C_6	1.5311	1.5298	1.5388	1.5359	1.5273	1.5221
C_2C_6	1.5513	1.5529	1.5493	1.5507	1.5535	1.5594
C_2O_{13}	1.2432	1.2793	1.2428	1.2757	1.2365	1.2689
$O_{13}H_{14}$	3.3088	2.9608	1.9397	1.8536	5.1003	5.1045
$O_1C_2N_3$	133.9	142.9	177.1	176.3	119.8	119.9
$O_1C_2C_6$	115.0	115.2	115.3	115.8	114.6	114.7
$C_2N_3N_4$	58.1	61.0	75.1	76.2	57.7	58.5
$N_3N_4C_5$	111.1	108.7	116.6	115.2	111.7	109.7
$O_{13}C_2N_3$	80.3	73.4	49.3	48.9	110.5	110.2
$H_{14}O_{13}C_2$	75.3	82.5	119.6	118.1	45.5	45.2
O_1C_2-N_3N_4	186.9	193.8	161.4	161.5	155.4	156.1
$H_7C_2-N_3N_4$	77.0	77.8	258.6	259.5	25.1	25.6
$H_8C_2-N_3N_4$	31.7	32.0	30.0	30.5	31.1	31.4
C_2N_3-N_4C_5	57.7	56.8	29.9	28.3	21.1	21.0
O_1C_2-C_5C_6	1.8	21.7	311.3	309.6	25.7	27.1
$O_{13}C_2$-N_3N_4	52.0	62.1	184.3	186.3	326.3	326.8
energy	−376.3106524	−377.4391535	−376.3092213	−377.4372310	−376.3019867	−377.4281246
ZPE	0.122714	0.109571	0.122607	0.109476	0.121751	0.108711
no. of imag freq	0		0		0	

[a] Bond lengths in angstroms, bond and dihedral angles in degrees, and energy in hartrees.

TABLE 4: MP2 Relative Energies and Barrier Heights (in kcal/mol) of the Principal Structures of the B_{AC2} and Elimination Reactions[a]

B_{AC2}	kcal/mol	elimination(1)	kcal/mol	elimination (2)	kcal/mol	elimination(3)	kcal/mol
a	0	**a**	0	**a**	0	**a**	0
b1	−33.04	**b1**	−33.04				
c1	−0.32	**g1**	−21.44				
b1 → c1	32.72	**b1 → g1**	11.60				
b2	−31.28			**b2**	−31.28		
c2	−5.64			**g2**	17.28		
b2 → c2	25.64			**b2 → g2**	48.56		
b3	−31.11						
b4	−29.54					**b4**	−29.54
d	−3.22	**h**	−35.18			**g3**	−24.25
						b4 → g3	5.29
f1	−56.71	**i1**	−33.79	**i2**	−12.36	**i3**	−35.66
f2	−55.56						
f3	−50.33						

[a] These values have been obtained using the ZPE-RHF energy sided by 0.8929.

As stated previously, solvent promotes a new activation energy, lower than 20 kcal/mol, in any case. This reveals that in γ-lactam compounds, even taking into account the former activation energy, the limiting step of the basic hydrolysis is the cleavage of the C−N bond. This conclusion totally agrees with the experimental results obtained by Bowden and Bromley,[29] who have indicated that for acetanilides and γ- and δ-lactam compounds the limiting step is the C−N bond fission. However, it should be stated that the activation energy we have theoretically obtained is slightly higher than that obtained by these authors.

Elimination Reaction. If the withdrawing process of the OH^- group from C_2 in the tetrahedral intermediates is studied without compelling this process to be perpendicular to the β-lactam ring, the system evolves spontaneously through an elimination mechanism. The reaction starts with the withdrawing of the OH^- group from the tetrahedral intermediate followed by the elimination of a proton of the γ-lactam ring to yield a water molecule (see Scheme 2). Analogous transition states are described in the literature, for both β-lactam[13] and *N*-methylcarbamate[30] compounds.

Transition state **g1**, obtained from tetrahedral intermediate **b1**, shows an energy barrier of 11.60 kcal/mol in relation to such intermediate (in MP2 calculations). This transition state is characterized by the presence of a hydrogen bond between H_8 and O_{13} (2.193 Å by RHF and 1.918 Å by MP2), and H_7 is located far from the hydroxyl group (3.551 and 3.678 Å in RHF and MP2 calculations, respectively, see Table 5). Therefore, the elimination reaction takes place with the H_8. The OH^- group is located below the $C_2N_3N_4$ plane with a dihedral angle of 65.0°, considerably far from perpendicularity. This structure has been characterized by vibrational analysis, showing an imaginary frequency involving the atoms C_2, O_{13}, and H_8.

MP2 calculations on this structure considerably approach the hydroxyl group to N_4 (from 2.193 Å in RHF to 1.918 Å in MP2) and withdraw this group from C_2 (from 2.112 to 2.321 Å). Therefore, this calculation shows up the hydrogen bond. The remaining bond distances increase between 0.01 and 0.03 Å, except the C_2C_6 distance that slightly decreases (0.002 Å).

IRC calculations on this structure end at the already known structure **b1** for the reverse pathway and at energy minimum **h** for the forward pathway (Figure 4, Table 5), in which the

TABLE 5: Main Geometric Parameters and Energies of the Transition States (g1, g2, g3), Intermediate (h), and Final Products (i1, i2, i3) of the Elimination

	structure **g1**		structure **h**		structure **i1**		structure **g2**		structure **i2**		structure **g3**		structure **i3**	
	RHF	MP2	RHF	MP2	RHF	MP2	RHF	MP2	RHF	MP2	RHF	MP2	RHF	MP2
O_1C_2	1.2097	1.2327	1.2088	1.2419	1.2274	1.2612	1.2248	1.2291	1.2523	1.2871	1.2243	1.2641	1.2487	1.2805
C_2N_3	1.4293	1.4383	1.3510	1.3658	1.3172	1.3428	1.4530	1.4331	1.4325	1.4590	1.3167	1.3288	1.2999	1.3320
N_3N_4	1.4116	1.4390	1.4234	1.4420	1.4358	1.4225	1.4304	1.4591	1.4282	1.4581	1.4262	1.4544	1.4397	1.4620
N_4C_5	1.4736	1.4896	1.4612	1.4766	1.4410	1.4555	1.4636	1.4816	1.4571	1.4892	1.4561	1.4845	1.4614	1.4817
C_5C_6	1.5346	1.5317	1.5344	1.5332	1.5385	1.5344	1.5215	1.5256	1.5093	1.5063	1.5223	1.5199	1.5189	1.5163
C_2C_6	1.5239	1.5261	1.5152	1.5161	1.5228	1.5261	1.5241	1.5155	1.3731	1.3851	1.5342	1.5428	1.5343	1.5403
C_2O_{13}	2.1122	2.3211	3.5065	3.4417	4.9660	4.9178	1.8957	2.5433	3.7402	3.3382	3.5011	3.4088	3.2898	3.2247
H_7-O_{13}	3.5505	3.6776	3.7502	3.7117	4.1820	4.1533	3.9642	4.0541	3.5392	2.6552	1.2546	1.1609	0.9527	0.9803
H_8-O_{13}	2.1929	1.9184	1.7620	1.6556	0.9751	1.0142	4.1462	4.5119	5.2042	4.2643	3.1222	3.3772	4.7205	4.6738
N_4-H_8	1.0024	1.0369	1.0269	1.0678	1.8922	1.7768	1.0001	1.0217	1.0104	1.0369	1.0002	1.0154	1.0002	1.0222
$O_{13}H_{14}$	0.9486	0.9765	0.9479	0.9745	0.9467	0.9709	0.9528	0.9769	0.9692	1.0084	0.9481	0.9721	0.9600	0.9903
$O_1C_2N_3$	121.2	122.2	125.8	125.7	128.1	127.9	117.7	121.2	118.7	118.7	128.8	128.4	128.0	127.5
$O_1C_2C_6$	125.4	126.2	128.1	128.7	127.0	128.4	127.7	128.8	134.2	134.5	123.1	122.2	121.3	122.1
$C_2N_3N_4$	128.2	107.8	113.8	114.1	117.1	117.9	106.4	107.0	108.3	107.1	104.8	109.7	108.5	107.2
$N_3N_4C_5$	106.9	105.2	101.1	99.7	99.7	99.0	107.3	105.5	101.2	99.4	104.8	105.6	106.6	105.3
$O_{13}C_2N_3$	91.3	86.9	72.9	72.9	35.6	35.9	100.9	99.6	93.7	79.6	29.0	30.9	68.5	66.9
$H_{14}O_{13}C_2$	101.6	100.5	144.9	143.9	101.4	100.5	115.0	124.8	14.8	26.2	97.6	85.8	41.4	40.4
O_1C_2-N_3N_4	182.2	177.6	170.9	171.1	174.6	175.2	199.3	198.0	198.5	199.6	173.3	170.0	175.5	174.1
H_7C_2-N_3N_4	239.3	239.2	148.2	147.3	169.8	170.5	244.7	239.5	234.9	238.6	155.8	132.3	173.3	165.2
H_8C_2-N_3N_4	31.8	32.1	30.2	30.5	31.1	29.8	343.1	338.1	331.5	322.4	339.2	335.6	337.7	352.0
C_2N_3-N_4C_5	28.6	30.4	30.6	30.8	25.1	23.8	30.1	24.1	325.4	322.1	30.3	25.9	25.7	28.3
O_1C_2-C_5C_6	313.4	314.9	315.9	312.4	313.4	308.3	133.9	273.7	27.8	36.4	319.1	333.7	320.2	316.9
$O_{13}C_2$-N_3N_4	65.0	60.6	43.8	42.9	15.9	29.8	76.3	82.0	219.0	231.7	153.7	161.9	174.2	166.8
energy	−376.2356359	−377.3807251	−376.2611738	−377.4014815	−376.2572457	−377.3974855	−376.1735520	−377.3166547	−376.2324123	−377.3652351	−376.2377132	−377.3810772	−376.2904964	−377.4027356
ZPE	0.120216	0.107341	0.118948	0.106209	0.116960	0.104434	0.117571	0.104979	0.119077	0.106324	0.115546	0.1032156	0.119504	0.106705
no. of imag freq	1 (268.77*i*)		0		0		1 (491.88*i*)		0		1 (1196*i*)		0	

[a] Bond lengths in angstroms, bond and dihedral angles in degrees, energy in hartrees, and imaginary frequencies in cm^{-1}.

SCHEME 2: Scheme of the Elimination Reactions

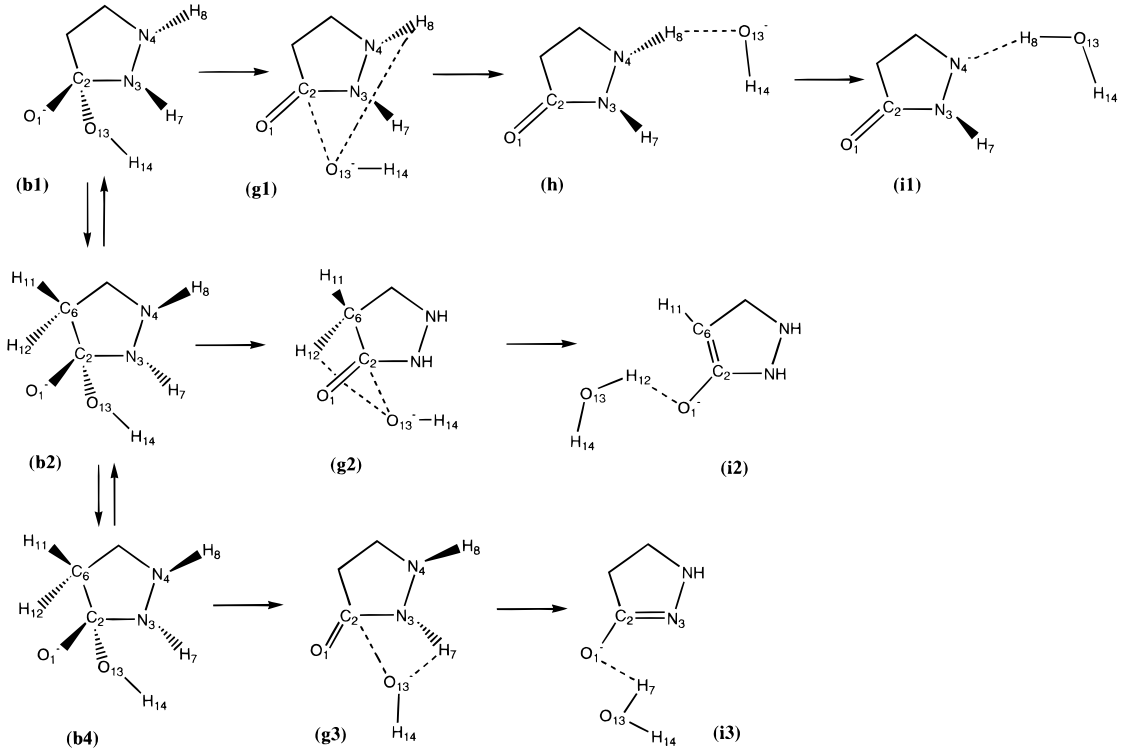

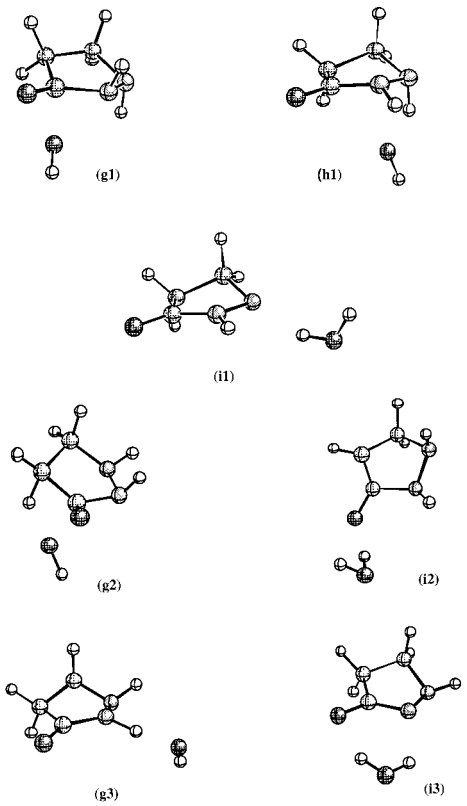

Figure 4. Structures corresponding to the intermediates of the elimination reactions.

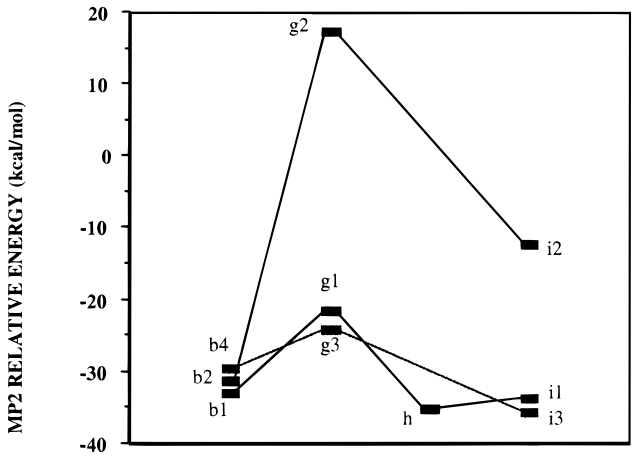

Figure 5. Reaction profile of elimination reactions.

hydroxyl group is very far from the carbonyl group (C_2O_{13} distance of 3.507 Å in RHF calculations) and with a hydrogen bond between the H_8 and the O_{13} atoms (1.762 Å). Once more, MP2 calculations decrease the length of the hydrogen bonds (H_8O_{13} distance of 1.656 Å).

In the intermediate **h**, H_7 is located considerably far from O_{13} (3.750 and 3.712 Å in RHF and MP2 calculations, respectively), and the hydroxyl group is found in the appropriate situation to eliminate H_8 of the ring (distance H_8O_{13} of 1.762 and 1.656 Å in RHF and MP2 calculations, respectively). If a reaction coordinate is performed approaching H_8 to the hydroxyl ion, it is observed the elimination of this hydrogen with formation of water (structure **i1**, Figure 4, Table 5). Therefore, the transition state **g1** is a cross between the basic hydrolysis reaction and the elimination reaction. The elimination takes place without virtually any energy activation, as expected,[16] and no transition state has been found. The reaction profile corresponding is plotted in Figure 5, and activation energies are given in Table 4. The final reaction product presents an energy higher than the tetrahedral intermediate and, moreover, considerably higher than the final product of the alkaline hydrolysis (**f1**). The energy difference between the final product of the elimination reaction and the reagents is of −26.52 kcal/mol (RHF) and slightly larger by MP2 calculations (−33.79 kcal/mol).

From tetrahedral intermediate **b2** and **b4** two different final products can be obtained depending on the eliminated proton.

H_{12} elimination from **b2** yields product **i2** through transition state **g2**, and H_7 elimination from **b4** gives rise to the final product **i3** through transition state **g3**. Both transition states have been characterized by vibrational study.

Table 5 shows the main geometric parameters of these final products and transition states. As can be seen in this table, the most stable product is **i3**.

Acknowledgment. The authors wish to thank the Centre de Càlcul de la Universitat de les Illes Balears for access to their computer facilities. We are indebted to Dr. Michael W. Schmidt for providing us a copy of his version of the GAMESS program. The support of the Spanish DGICYT is gratefully acknowledged (Project PB96-0596-C02-02).

References and Notes

(1) Chamber, R. B. *Chemistry and Biology of β-lactam Antibiotics*; Academic Press: New York, 1982; Vol. 3, pp 287−300.

(2) Harada, S.; Tsubotani, S.; Hida, T.; Koyama, K.; Kondo, M.; Ono, H. *Tetrahedron* **1988**, *44*, 6589.

(3) Jungheim, L. D.; Sigmund, S. K.; Fisher, J. W. *Tetrahedron Lett.* **1987**, *28*, 285.

(4) Allen, N. E.; Hobbs, J. N.; Preston, D. A.; Turner, J. R.; Yu, C. Y. E. *J. Antibiotics* **1990**, *43*, 92.

(5) Baldwin, J. E.; Lynch, G. P.; Pitlik, J. *J. Antibiotics* **1991**, *44*, 1. Boyd, D. B. *J. Med. Chem.* **1993**, *36*, 1443.

(6) Boyd, D. B. *Chemistry and Biology of β-lactam Antibiotics*; Academic Press: New York, 1982; Vol. 1, pp 437−545 and references cited there.

(7) Vishveshwara, S.; Rao, V. S. R. *J. Mol. Struct. (THEOCHEM)* **1993**, *92*, 19.

(8) Alcolea Palafox, M.; Nuñez, J. L.; Gil, M. *J. Phys. Chem.* **1995**, *99*, 1124.

(9) Fernandez, B.; Carballeira, L.; Rios, M. A. *Biopolymers* **1992**, *32*, 97.

(10) Frau, J.; Coll, M.; Donoso, J.; Muñoz, F.; Garcia Blanco, F. *J. Mol. Struct. (THEOCHEM)* **1991**, *231*, 109.

(11) Smeyers, Y. G.; Hernandez-Laguna, A.; Gonzalez-Jonte, R. *J. Mol. Struct. (THEOCHEM)* **1993**, *287*, 261.

(12) Frau, J.; Donoso, J.; Muñoz, F.; Garcia Blanco, F. *Helv. Chim. Acta* **1994**, *77*, 1557.

(13) Frau, J.; Donoso, J.; Muñoz, F.; Garcia Blanco, F. *Helv. Chim. Acta* **1996**, *79*, 353.

(14) Coll, M.; Frau, J.; Donoso, J.; Muñoz, F. *J. Mol. Struct. (THEOCHEM)*, in press.

(15) Frau, J.; Coll, M.; Donoso, J.; Muñoz, F.; Vilanova, B.; Garcia Blanco, F. *Electron. J. Theor. Chem.* **1997**, *2*, 56.

(16) Pranata, J. *J. Phys. Org. Chem.* **1996**, *9*, 711. Pranata, J. *J. Phys. Chem.* **1994**, *98*, 1180. O'Brien, J. F.; Pranata, J. *J. Phys. Chem.* **1995**, *99*, 12759.

(17) Pitarch, J.; Ruiz-López, M. F.; Pascual-Ahuir, J. L.; Silla, E.; Tuñon, J. *J. Phys. Chem. B* **1997**, *101*, 3581.

(18) Frau, J.; Donoso, J.; Muñoz, F.; Vilanova, B.; Garcia Blanco, F. *Helv. Chim. Acta* **1997**, *80*, 739.

(19) Fisher, J. *Antimicrobial Drug Resistance: β-lactam Resistant to Hydrolysis by the β-lactamases*; Academic Press: New York, 1984.

(20) Flynn, E. H. *Cephalosporins and Penicillins: Chemistry and Biology*; Academic Press: New York, 1972. Nishikawa, J.; Tori, K. *J. Med. Chem.* **1984**, *27*, 1657.

(21) Indelicato, J. M.; Passini, C. E. *J. Med. Chem.* **1988**, *31*, 1227.

(22) Madura, J. D.; Jorgensen, W. L. *J. Am. Chem. Soc.* **1986**, *108*, 2517.

(23) Moller, C.; Plesset, M. S. *Phys. Rev.* **1934**, *46*, 618.

(24) Pople, J. A.; Binkley, J. S.; Seeger, R. *Int. J. Quantum Chem.* **1976**, *510*, 1. Pople, J. A.; Seeger, R.; Krishnan, R. *Int. J. Quantum Chem.* **1977**, *511*, 165.

(25) Pople, J. A.; Schlegel, H. B.; Krishnan, R.; DeFrees, D. J.; Binkley, J. S.; Frisch, M. J.; Whiteside, R. A.; Hout, R. F.; Hehre, W. *Int. J. Quantum Chem., Quantum Chem. Symp.* **1981**, *15*, 269.

(26) Dupuis, M.; Spangler, D.; Wendolowski, J. J. *'GAMESS US'*, National resources for Computations in Chemistry, Software Catalog, Vol 1, **1980** Program QGO1, Lawrence Berkley Laboratory, USDOE, California.

(27) Schmidt, M. W.; Baldridge, K. K.; Boatz, J. A.; Elbert, S. T.; Gordon, M. S.; Jensen, J. H.; Koseki, S.; Matsunaga, N.; Nguyen, K. A.; Su, S. J.; Windus, T. L.; Dupuis, M.; Montgomery, J. A. *J. Comput. Chem.* **1993**, *14*, 1347.

(28) Frau, J.; Donoso, J.; Muñoz, F.; Garcia Blanco, F. *J. Comput. Chem.* **1993**, *14*, 1545.

(29) Bowden, K.; Bromley, K. *J. Chem. Soc., Perkin Trans. 2* **1990**, 2103. Bowden, K.; Bromley, K. *J. Chem. Soc., Perkin Trans. 2* **1990**, 2111.

(30) Katagi, T. *J. Comput. Chem.* **1990**, *11*, 524.